Soft Matter

Accepted Manuscript

ROYAL SOCIETY OF CHEMISTRY

www.rsc.org/softmatter

Liquid crystalline assembly of rod-coil diblock copolymer and homopolymer blends by dissipative particle dynamics simulation

Huihui Wu[1], Linli He[1,*], Xianghong Wang[2] , Yanwei Wang[1], and Zhouting Jiang[3]

[1]*Department of Physics, Wenzhou University, Wenzhou 325035, P R China*

[2]*Wenzhou Vocational & Technical College, Wenzhou 325035, P R China*

[3] *China Jiliang University, Hangzhou 310027, P R China*

[*] Corresponding author. Electronic mail: linlihe@wzu.edu.cn

The liquid crystalline assembly of rod-coil diblock copolymers blended with coil or rod homopolymers is investigated using the dissipative particle dynamics simulation, considering systematically the effect of the interactions between rods and coils, the volume fraction and length of the added coil or rod homopolymers. The addition of coil or rod homopolymers induces disorder-order or order-liquid crystalline transition. In rod-coil/coil blends, the solubilization of homopolymers will saturate at a certain amount of homopolymers and then the excess homopolymers will be segregated into the central regions of coil block domains, forming "wet-dry mixture" lamellae. The solubility capacity decreases with homopolymer length increasing, determined by the competition between mixing entropy and elastic entropy. In rod-coil/rod blends, due to the orientational interactions between rods, the length matched rod homopolymers directly interdigitate with rod blocks with less entropy loss, thus prompting the formation of bilayer liquid crystalline phase. The rods domain spacing D_r remains unchanged and conversely the coils domain spacing D_c becomes thin, to occupy more interfacial area. With the addition of shorter rod homopolymers, the overall lamellar spacing D of blends monotonically increases with the volume fraction of homopolymers, similar to the case of rod-coil/coil blends. Generally, rod homopolymers have a more significant impact on the liquid crystalline assembly of the blends, compared with the coil homopolymers. Our results indicate that blending with coil or rod homopolymers into rod-coil system is an effective method to induce liquid crystal phase transition and control the phase spacing of ordered structure.

1. Introduction

Recently, more attention has been given to rod-coil block copolymers which consist of rigid rod blocks and flexible coil blocks, because it represents a unique polymeric system with various morphologies and practical applications, such as organic optoelectronic, electrochemical and biotechnology.[1] In contrast to traditional coil-coil block copolymers, the phase behavior of rod-coil block copolymers is obviously complex due to both the conformational asymmetry between rod and coil blocks, and the orientational interaction between anisotropic rods, as well as the volume fraction of the coil blocks and the Flory-Huggins interaction. Previous studies have reported complex phases including isotropic, nematic, smectic (A and C) liquid crystalline, zigzag, wavy, and perforated lamellae as well as the conventional lamellae, cylindrical, and spherical phases.[2-5]

Furthermore, adding homopolymers into block copolymer systems has been an effective method for controlling phase domain size, tailoring morphology, and optimizing performance without additional synthesis.[6-8] The morphology of blends become more complicated than the pure block polymers, but it is expected to be rich, since there is an interplay between "microphase separation", i.e., between coil and rod blocks, and "macrophase separation", i.e., between copolymers and homopolymers. As in traditional coil-coil diblock copolymer systems (i.e., A-*b*-B), rich morphologies of A-*b*-B diblock copolymers can be induced by mixing with a certain amount of homopolymers (such as A component). The phase behaviors of the blending system depend not only on the volume fraction and specie of added homopolymers, but also on the ratio of the molecular weight of added homopolymer to that of corresponding block in diblock copolymers, which can be expressed by the parameter α, indicating the permeating degree of added homopolymers into diblock copolymer matrix. Referring to the studies by Tanaka[9] and analysis by Lai,[10] when $\alpha < 1$, the short A homopolymers are solubilized thoroughly and distributed uniformly into A microdomain to swell the distance between the junction points at the domain interface, which is known as "wet-brush"; when $\alpha \approx 1$, i.e., the size of added homopolymers is matched to one of the blocks, which is the simplest and most studied case. A homopolymers are also solubilized into A microdomains and just centrally located in the middle regions of A domains, which is named as "dry-brush"; finally, when $\alpha > 1$, "macrophase separation" between A

homopolymer phase and A-*b*-B diblock microdomain phase may occurs.

It is conceivable that the phase behavior of rod-coil block copolymers is also rich and complicated, by mixing with the homopolymers (coils or rods), due to the interplay between "microphase separation" and "macrophase separation", as well as the orientational interaction between anisotropic rods, and the conformational asymmetry between rods and coils. Recently, only a few studies begin to pay attentions to this blending system, which consists of rod-coil block copolymers and coil or rod homopolymers.[10-16] For instance, Lai et al. experimentally studied the phase behaviors of strongly segregated PPV-b-PMMA diblock copolymers blended with PMMA homopolymers (coils). Over the major composition range, the blends underwent macrophase separation irrespective of the ratio of molecular weight of homopolymer relative to that of corresponding block. A well-ordered lamellar morphology and a sponge structure appeared in microphase separation.[10] Sary et al. investigated the blends of PPV-b-PS diblock copolymers and PPV homopolymers(rods), which had the same molecular weight with the rod block of PPV-b-PS diblocks. With adding PPV homopolymers, the morphology of weakly segregated rod-coil diblock copolymers was transited from an isotropic homogeneous phase to a smectic-C bilayer lamellar clusters.[12] Tao et al. also found that the domain size of lamellar PPV-b-PI could be controlled by blending with PI or PPV homopolymers, whose molecular weight was the same as the corresponding blocks in PPV-b-PI copolymers. They observed that the domain size was increased by the solubilization of PI homopolymers within coil block microdomain; while it was decreased by the interdigitation of PPV homopolymers within rod block domains.[13] Song et al. used a hybrid self-consistent field theory (SCFT) to construct the phase diagrams of the blends as a function of the homopolymer volume fraction and phase segregation strength. They found that both coil and rod homopolymers could enhance the stability of ordered phases.[14]

Nevertheless, most experiment and theory studies on rod-coil block copolymers and homopolymers blends, especially for rod homopolymers, are limited to the case that the molecular weight of homopolymer is matched with that of corresponding block in block copolymers. In this paper, we firstly utilize dissipative particle dynamics (DPD) simulation to investigate the self-assembly behavior of rod-coil/coil and rod-coil/rod blends under weakly and strongly segregated conditions, respectively. We detect the phase transition and domain spacing of the blends varied by the repulsive interaction between rod and coil component, the coil or rod

homopolymer length and volume fraction, and meanwhile reveal the physical mechanisms of the disorder-order and order-liquid crystalline transitions.

2. Model and simulation method

The DPD method was introduced by Hoogerbrugge[17] in 1992, is a simulation technique which can treat a wider range of length and time scales compared to atomistic simulations like classical molecular dynamics (MD). Within DPD, a particle represents the center of mass in a cluster of atoms, and the position and momentum of the particles are updated by Newton's equation of motion. Particles i and j at positions $\vec{r}_i$ and $\vec{r}_j$ interact with each other via three forces: conservative($\vec{F}^C$), dissipative($\vec{F}^D$) and random forces($\vec{F}^R$). The sum acts ($\vec{f}_{ij} = \vec{F}_{ij}^C + \vec{F}_{ij}^D + \vec{F}_{ij}^R$) over all beads within a cutoff radius r_c beyond which the forces are neglected. Typically, the conservative force $\vec{F}^C$ for non-bonded beads becomes zero outside the cutoff radius r_c.

$$\vec{F}_{ij}^C = a_{ij}\omega(r_{ij})\hat{r}_{ij} \quad (1)$$

$$\vec{F}_{ij}^D = -\gamma\omega^2(r_{ij})(\hat{r}_{ij}\cdot\vec{v}_{ij})\hat{r}_{ij} \quad (2)$$

$$\vec{F}_{ij}^R = \sigma\omega(r_{ij})\theta_{ij}\hat{r}_{ij} \quad (3)$$

$$\omega(r) = \begin{cases} 1 - r_{ij}/r_c & r_{ij} < r_c \\ 0 & r_{ij} \geq r_c \end{cases} \quad (4)$$

where $\vec{r}_{ij} = \vec{r}_i - \vec{r}_j$, $r_{ij} = \left|\vec{r}_{ij}\right|$, $\hat{r}_{ij} = \vec{r}_{ij}/r_{ij}$, and $\vec{v}_{ij} = \vec{v}_i - \vec{v}_j$. The coefficients a_{ij}, γ and σ define the strength of conservative, dissipative, and random forces, respectively. The relation between the coefficients γ and σ as follows:

$$\sigma^2 = 2\gamma k_B T \quad (5)$$

where k_B is Boltzmann's constant. Additionally, θ_{ij} in Eq.(3) is a randomly fluctuating variable with Gaussian statistics: $\langle\theta_{ij}(t)\rangle = 0$ and $\langle\theta_{ij}(t)\theta_{kl}(t')\rangle = (\delta_{ik}\delta_{jl} + \delta_{il}\delta_{jk})\delta(t-t')$. In order to match the compressibility of water requiring,[18,19]

$$a_{ii}\rho = 75k_BT \qquad (6)$$

a_{ii} is the repulsion parameter between particles of the same type. Similar to the classic DPD studies on rod-coil system by AlSunaidi, et. al.,[20] in our study the particle density ρ is kept to 4, so the conservative strengths a_{ij} between DPD beads (represented by r and c) are given by $a_{cc} = a_{rr} = 20$ and the variable a_{rc} For coil blocks, we have to consider the spring force $\vec{F}_i^S = C\vec{r}_{ij}(C = 4)$, where C is the spring constant. For rod blocks, it can be constructed by a number of DPD beads arranged in a straight line, with a fixed small distance D_{b-b} between consecutive beads.[20-22] Here we set D_{b-b} as 0.3. For simplicity, L_c and L_r are used to represent the length of coil and rod homopolymers, respectively. In DPD simulation, all the physical variables are scaled by the particle mass m, cutoff distance r_c, and thermal energy k_BT. For example, the time, length and interaction parameter of system are nondimensionalized by $t = \frac{t'}{\sqrt{mr_c^2 / k_BT}}$, $r = \frac{r'}{r_c}$, and $a_{ij} = \frac{a_{ij}^{'}}{(k_BT / r_c^2)}$ where the superscript "′"denotes the dimensional variable. All the parameters listed in this work are dimensionless quantities and their physical values can be straightforwardly obtained.

It is worth mentioning that our simulation is performed in a constant NVT ensemble rather than NPT ensemble[20], because the simulation with NVT ensemble is more computationally efficient and easy to control. To confirm that the NVT ensemble is not a factor to cause the artificial phases, some critical points in the phase diagram are also simulated with the NPT ensemble using Berendsen barostat method[23], which shows no obvious difference between that obtained from NVT ensemble and NPT ensemble. Simulations are performed in a cubic box under periodic boundary conditions in three different directions. To void the finite size effects, we have investigated three simulated systems with different sizes of $15\times15\times15$, $20\times20\times20$, and $25\times25\times25$ DPD units, by quantitatively comparing the ordered parameters of system, such as lamellar period, which shows the same results. In the following, we focus on the box of $25\times25\times25$, containing about 62500 DPD particle (represented by N) with the melts

density ρ=4 . The volume fraction of the added coil homopolymers and rod homopolymers are expressed as $\phi_c = \frac{N_c}{N + N_c}$ and $\phi_r = \frac{N_r}{N + N_r}$, where N_c and N_r represent the particle number of added homopolymers. The blending system starts from a random initial distribution and mix. The time integration of motion equations is calculated through a modified velocity–Verlet algorith[18] with time step $\Delta t = 0.04$ and $\lambda = 0.5$. The typical simulation requires at least 1.0×10^6 step and the first 0.8×10^6 step is used for ensuring equilibrium(corresponding to about $1\mu s$ for typical physical values of the parameters). Actually, the system has been basically stable after 0.4×10^6 step. In addition, we also checked the thermodynamic consistency of simulated structures by monitoring the local temperature and pressure,[24] to ensure the acquirement of every equilibrium structure.

3. Results and discussion

A. Rod-coil block copolymer melts

It is known that the presence of the rod component breaks the symmetry of bulk phase diagram of block copolymer, which exists in coil-coil diblock copolymer. As the studies by Li, et al.[25] and An, et al.[26] on rod-coil diblock copolymer melts using the self-consistent-field (SCF) lattice model, lamellae occupies dominantly the phase diagram with high rod composition (i.e., $f_r \geq 0.5$). However, the conventional lamellae and liquid-crystalline (LC) lamellae phase were not distinguished in their phase diagram. In this paper, we focus on the liquid crystalline assembly of rod-coil diblock copolymers blended with corresponding coil or rod homopolymers. Typically, we select the linear R_8C_6 diblcok copolymer for study, where lamellae phase can be maintained even blended with a large amount of corresponding homopolymers. Here, the ordered lamellae structure distinguished from disordered phase is identified easily by component density distribution. For example, as the peak value of rods corresponds to the valley value of coils, as a result, it is a well ordered lamellae, including the liquid crystalline lamellae. To further distinguish between lamellar phase and liquid crystalline lamellae, we also need to monitor the rod orientation behaviors in detail.

Firstly, we simply construct the phase diagram of R_8C_6 melts as the function of the repulsive interactions between blocks rod and coil a_{rc}. Varying the interaction a_{rc} from 20 to 80, the simulated equilibrium morphologies are shown in Fig.1. The critical point for R_8C_6 morphology occurs at around $a_{rc} = 23$, which is close to the disorder-order transition. With increasing a_{rc} beyond the critical point, the disordered homogeneous phase is transited into lamellae phase (e.g., $a_{rc} = 25$), and further the lamellae with partially bilayer crystalline characteristic within rod block domains (e.g., $a_{rc} = 50$ and 75) is observed. In the following, we consider the two blends of rod-coil/coil and rod-coil/rod with different phase segregation strengths a_{rc}. For simplicity, we define both weakly segregated(a_{rc} = 23) and strongly segregated(a_{rc} = 50) systems, respectively.

B. Weakly Segregated system with a_{rc} = 23

Rod-coil/coil Blends:

In accordance with the polymer brush theories[27, 28] applied to the traditional coil-coil/coil blends, the shorter coil homopolymers are uniformly solubilized into the coil block domains formed "wet-brush". While the coil homopolymer length is the same or longer than that of the coil block, homopolymers are also solubilized and tend to be segregated in the central regions of the coil block domains formed "dry-brush". Fig.2a shows the phase diagram of rod-coil/coil blends for a_{rc}=23 plotted as a function of ϕ_c and L_c. It is clear that the diagram includes three phase regions, i.e., disorder, lamellae(wet), and lamellae(wet-dry). As is known, the solubilization of coil homopolymers in blocks can effectively relax the stretching conformational entropy of coils, which promotes the disorder-lamellar transition. Distinguished from the case of coil-coil/coil blends, the solubilization will saturate at a certain amount of coil homopolymers mixed into rod-coil system, which was also observed by the experimental study of Lai et al.[10] and Zin et al.[11] Due to the presence of solubility limit, the excess coil homopolymers will tend to be expelled and distributed in the central coil block domain, together leading to the formation of "wet-dry" mixture type. From the figure, we also can see that the phase boundaries of disorder-lamellae transition shift to a lower ϕ_c as L_c increases. It indicates that the solubility capacity decreases with

increasing L_c (i.e., molecular weight of homopolymer), which depends on the competition between mixing entropy and elastic entropy.[11] Fig.2b displays representative simulated morphologies of the blends for L_c = 6. We monitor the mixing behavior of coil homopolymers in copolymer matrix through the density distribution profile of each component[26,27]. For example, as ϕ_c=0.09, coil homopolymers are uniformly distributed in the overall coil block domains, where the observed lamellae structure is "wet" type. As ϕ_c increases to 0.15, the excess of coil homopolymers are mainly segregated in the center of the coil block domains formed "wet-dry" mixture within lamellae, where coil homopolymers distribution has a peak value in coil block domains, significantly different from wet layers.

Rod-coil/rod Blends:

Fig.3a presents the phase diagram of rod-coil/rod blends for a_{rc}=23, plotted as ϕ_r vs L_r, which includes disorder, lamellae, and liquid crystalline structure. In this case of rod-coil/rod system, the mixing of rod homopolymers can increase the effective interaction between the rod blocks and induce ordering within the blocks.[29] With the addition of rod homopolymers, the morphology of blends is easily transited from the disordered phase to lamellae. Similarly, the critical point of ϕ_r decreases with the increase of L_r. Furthermore, when L_r is close to the length of rod block, i.e. $L_r \approx 8$, liquid crystalline lamellae with a bilayer structure appears. In fact, the addition of rod homopolymers increases equivalently the rod composition in the blends system.[12] As it reaches to a high composition of rod component (e.g., $f_r \geq 0.7$), liquid crystalline phase will occupy dominantly the phase region, consistent with the studies on rod-coil system.[23] Substantively, the orientational interactions between anisotropic rods can lead to an aggregation between rod blocks and rod homopolymers. The rod blocks tend to be aligned along a common direction, and meanwhile rod homopolymers interdigitate with rod blocks to make coil blocks rearrange, to occupy more laterally interfacial area. To decrease the interfacial energy, a bilayer liquid crystalline phase is formed. Similarly, we draw the phase transition boundary by further monitoring the orientation behaviors between anisotropic rods. Fig.3b displays the typical

simulated morphologies of rod-coil/rod blends for L_r = 8. As ϕ_r = 0.01, the morphology is still disorder. Lamellae structure occurs when ϕ_r equals to 0.05. With increasing ϕ_r, the liquid crystalline phase gradually appears, e.g., ϕ_r = 0.15, and finally a well bilayer smectic-A liquid crystalline lamellae is observed with ϕ_r = 0.21.

To observe the effect of rod homopolymers on the phase transition and interdomain distance of rod-coil/rod blends, Fig.3c shows the lamellar spacing D (marked in Fig.3b) in lamellae-liquid crystalline transition with ϕ_r for both L_r = 2 and L_r =8 cases. As can be seen that when L_r is the same to that of rod blocks, D firstly increases, while it levels off at ϕ_r ~0.19. The results reveals that the rod homopolymers interdigitate with rod blocks to form a bilayer liquid crystalline phase and thus stabilize the lamellar spacing D. Whereas the shorter rod homopolymers (L_r = 2) are incorporated into rod block regions and do not align well, there is lamellae structure observed without liquid crystalline phase. Thus the lamellar spacing D is monotonously swollen with the increase of ϕ_r.

C. Strongly Segregated system with a_{rc} = 50

Rod-coil/coil Blends:

We also investigate the strongly segregated case of rod-coil/coil blends. As shown in Fig.1, a well lamellae structure is observed for R_8C_6 melts at a_{rc} = 50. Fig.4a displays the lamellae-liquid crystalline transition diagram by ϕ_c vs L_c, which indicates that the addition of coil homopolymers not only stabilizes ordered morphology, but also induces the formation of liquid crystalline structure. Moreover, liquid crystalline phase requires a lower ϕ_c as L_c is increased. In detail, Fig.4b exhibits the simulated morphologies of rod-coil/coil blends for L_c =6. Obviously, with the addition of coil homopolymers, lamellae structure is transformed into bilayer smectic-A liquid crystalline phase. Based on the above discussion on wet/dry behavior of coil homopolymers in rod-coil/coil blends, as the increase of ϕ_c, the excess coil homopolymers tend to aggregate into the central domains of coil blocks. Then coil homopolymers have to stretch along the direction

normal to the interface, resulting in the decrease of the interfacial area of coil blocks domain. As a result, the orientational interactions between rod components drive them to interdigitate with each other to enlarge the interfacial area for coil-stretching entropy, consequently giving rise to the liquid crystalline phase. In contrast to the SCF results of monolayer liquid crystalline obtained by Song et al.,[14] here the bilayer phase mainly results from the self-assembling characteristic of selected rod-coil melts, as shown in Fig.1.

To better understand the liquid crystalline assembly of rod-coil copolymers blended with corresponding homopolymers, we detect the variation of interdomain distance (i.e., lamellar period) with the addition of homopolymers. Fig.4c displays the lamellar spacing D as a function of ϕ_c for L_c = 2, 6, and 10, respectively. As a whole, the overall lamellar distance D increases with ϕ_c. It can be seen that for the same ϕ_c, D increases slightly with the increase of L_c, indicating the solubilization behavior of coil homopolymers depends on L_c, which is analogous to the case of coil-coil/coil blends.[29-31] The inset of Fig.4c also provides the domain spacing of the blends including coils spacing (D_c), rods spacing (D_r) and the overall lamellae period ($D = D_c + D_r$) (marked in Fig.4b) for L_c = 6. With the addition of coil homopolymers, rod domain spacing D_r increases slightly at first, and then it keeps unchanged, due to the formation of liquid crystalline phase resulted from the intrinsic rigidity and orientational interactions between rods. On the contrary, the coils domain D_c are monotonically swollen with ϕ_c.

Rod-coil/rod Blends:

Here we pay attention to rod-coil/rod blends under the strongly segregated condition (a_{rc} = 50). As shown in Fig.5a, liquid crystalline phase also appears upon the addition of rod homopolymers with L_r = 5~8. Similar to the case of weakly segregated system, the shorter rod homopolymers ($L_r \leq 4$) also tend to aggregate without alignment in rod block domains. However, the difference is liquid crystalline phase already appears at L_r = 5 for the case of strong

interaction, which indicates that the interaction a_{rc} also plays an important role on the liquid crystalline assembly of blends. Fig.5b illustrates the example of L_r = 8 in detail. With incorporation of rod homopolymers, rod block domains tend to expand along the direction normal to the interface, causing a contraction of the conformation of coil chains in the direction normal to the interface.[31] As a result, to balance the competition between coil stretching entropy and interfacial energy, the rods tend to interdigitate with each other including rod homopolymers, to form a bilayer liquid crystalline phase.

The lamellar spacing of rod-coil/rod blends for L_r = 2 and 8 cases are shown in Fig.5c, where the domain spacing (D, D_c, D_r) for L_r =8 are presented in the insert. Similar to the results of weakly segregated case shown in Fig.3c, the lamellar spacing D for shorter rod homopolymers(L_r = 2) is increased with the solubility of rod homopolymers, while for L_r = 8, it increases firstly and then levels off. Finally, upon adding excess rod homopolymers, liquid crystalline phase is formed. Interestingly, it is known that the added rod homopolymers expand the rod-coil laterally interfacial width, and then it requires the coils to rearrange along the increased laterally interfacial area, resulting in a contraction of the thickness of coil blocks along the direction of interface.[13] Therefore, the coils spacing D_c decreases slightly as the addition of rod homopolymers, shown in the insert of Fig.5c. The similar results are also observed in the experiment on rod-coil-rod triblock copolymers/rod homopolymers by Gao et al.[15]

Finally, to further compare the effects of coil or rod homopolymers on the liquid crystalline assembly of rod-coil system, we calculate the rod orientation distribution $p(\cos\theta)$ as a function of $\phi_{\mathrm{hom}o}$ (i.e., ϕ_c or ϕ_c), where θ is the included angle between two neighboring rods. When $p(\cos\theta)$ is close to 1.0, i.e. θ approaching to 0°, indicating a perfect alignment between rods; for $p(\cos\theta)$ is close to 0, rods have a completely disordered arrangement. Corresponding to the two insets of Fig.4c and Fig.5c, we consider the both length matched cases of R_8C_6/C_6 and R_8C_6/R_8 blends. As clearly shown in Fig.6, $p(\cos\theta)$ for rod homopolymers increases faster and liquid crystalline phase with $p(\cos\theta) \approx 1.0$ appears earlier than that of coil homopolymers case. It suggests that adding rod homopolymers can orient the alignment of rods and induce the liquid

crystalline phase better. Substantively, the addition of rod homopolymers equivalently increases the rod composition. Furthermore, due to the orientational interactions between rods, the length matched rod homopolymers directly interdigitate with rod blocks with less entropy loss, thus prompting the formation of liquid crystalline phase. However, coil homopolymers are solubilized into coil block domains first, and then indirectly affects the orientational behaviors of rod blocks through interacting with coil blocks, i.e., entropy and enthalpy effects.

4. Conclusions

The liquid crystalline assembly of rod-coil diblock copolymers blended with coil or rod homopolymers is investigated using the dissipative particle dynamics simulation(DPD). We consider both weakly and strongly segregated cases for rod-coil/coil and rod-coil/rod blends, and examine the phase behavior of blends influenced by the volume fraction and length of coil or rod homopolymers. In general, the addition of coil or rod homopolymers can induce disorder-order or order-liquid crystalline transition. Compared to coil homopolymers, the addition of rod homopolymers can effectively improve the orientation of rods and induce the formation of liquid crystalline phase better.

For rod-coil/coil blends, the shorter coil homopolymers are uniformly solubilized into coil blcok domains formed "wet" lamellae. Interestingly, there is a solubilization limit as homopolymer length reaches a certain value, i.e., the solubilization of coil homopolymers will saturate with the addition of coil homopolymers, and then the excess homopolymers will be segregated into the central regions of coil block domains, together forming "wet-dry mixture" lamellae. Moreover, the solubility capacity decreases with increasing coil homopolymer length(i.e., molecular weight), which depends on the competition between mixing entropy and elastic entropy. For the strongly segregated case, upon the addition the coil homopolymers, bilayer liquid crystalline phase is observed, in which the overall lamellar spacing D is determined by the solubilization of coil homopolymers in corresponding block domains. The stability of rods domain spacing D_r indicates the formation of bilayer liquid crystalline phase.

For rod-coil/rod blends, with adding rod homopolymers, the disordered system is transited into lamellae and even bilayer liquid crystalline lamellae. This results can be attributed to the minimization of the free energy based on three energetic contributions: the energy gain due to the

rod-rod interactions, the interfacial energy between rods and coils, and the stretching energy of the coil blocks. Here, rod homopolymers can increase the energy gain arising from rods interactions, meanwhile decrease the rod-coil interfacial energy and the stretching energy of the coils. For shorter rod homopolymers, the lamellar spacing D monotonically increases with the incorporation of homopolymers, similar to the case of rod-coil/coil blends. For the length matched rod homopolymers, the rods domain spacing D_r increases slightly at first, and then keeps unchanged; Interestingly, rod homopolymers interdigitate with rod blocks expanding the rod-coil laterally interfacial width, and coil blocks are rearranged to occupy more interfacial area, resulting in a contraction of coil block domain spacing D_c along the direction of interface.

Acknowledgments

This research was financially supported by the National Natural Science Foundation of China (Nos. 21104060, 11304232, 31340026, 21204078 and 11372229) and the Natural Science Foundation of Zhejiang Province (LZ13F020003).

References

1 B. D. Olsen and R. A. Segalman, *Mater. Sci. Eng. R-Rep*. 2008, **62** (2), 37–66.

2 L. H. Radzilowski, B. O. Carragher, and S. I. Stupp, *Macromolecules* 1997, **30**, 2110-2119.

3 J. T. Chen, E. L. Thomas, C. K. Ober, and S. S. Hwang, *Macromolecules*, 1995, **28**, 1688-1697.

4 J. Z. Chen, C. X. Zhang, Z. Y. Sun, Y. S. Zheng, and L. J. An, *J. Chem. Phys.,* 2006, **124**, 04907.

5 P. T. He, X.J. Li, M.G. Deng, T. Chen and H. J. Liang, *Soft Matter*, 2010, **6**, 1539–1546.

6 N. V. Salim, N. Hameed, T. L. Hanley, and Q. P. Guo, *Soft Matter*, 2013, **9**, 6176-6184.

7 I. W. Hamley, The Physics of Block Copolymers. *Oxford University Press*: New York, 1998.

8 T. L. Morkved, B. R. Chapman, F. S. Bates, T. P. Lodge, P. Stepanek, and K. Almdal, *Faraday Discuss*, 1999, **112**, 335-350.

9 H. Tanaka, H. Hasegawa, and T. Hashimoto, *Macromolecules*, 1991, **24**, 240-251.

10 C. S. Lai, C. C. Ho, H. L. Chen, and W. F. Su, *Macromolecules*, 2013, **46**, 2249-2257.

11 S. H. Ji, W. C. Zin, N. K. Oh, and M. Lee, *Polymer*, 1997, **38**, 4377-4380.

12 N. Sary, R. Mezzenga, C. Brochon, G. Hadziioannou, and J. Ruokolainen, *Macromolecules*,

2007, **40**, 3277-3286.

13 Y.F. Tao, B. D. Olsen, V. Ganesan, and R. A. Segalman, *Macromolecules*, 2007, **40**, 3320-3327.

14 W. Song, P. Tang, F. Qiu, Y. Yang, and A. C. Shi, *J. Phys. Chem. B.*, 2011, **115**, 8390-8400.

15 L. Gao, J. Yao, Z. Shen, Y. Wu, X. Chen, X. Fan, and Q. Zhou, *Macromolecules*, 2009, **42,** 1047-1050.

16 N. P. Tzanetos, V. Dracopoulos, J. K. Kallitsis, and V. A. Deimede, *Langmuir,* 2005, **21**, 9339-9345.

17 P. J. Hoogerbrugge and J. M. V. A. Koelman，*Europhys Lett*. 1992, **19**(3), 155-160.

18 R. D. Groot and P. B.Warren, *J. Chem. Phys*., 1997, **107**, 4423-4435.

19 R. D. Groot and T. J. Madden, *J. Chem. Phys.*, 1998, **108**, 8713-8724.

20 B. A. AlSunaidi, W. K. den Otter, and J. H. R. Clarke, *Philos. Trans. R. Soc. London,* 2004, **362**,1773-1781.

21 M. J. A. Hore and M. J. Laradji, *J. Chem. Phys*., 2008, **128**, 054901.

22 B. A. AlSunaidi, W. K. den Otter, and J. H. R. Clarke, *J. Chem. Phys*., 2009, **130**, 124910.

23 Z.M. Zhang and H.X. Guo, *J. Chem. Phys*., 2010, **133**, 144911.

24 L.L. He, Z. L. Chen, R. F. Zhang, L. X. Zhang, and Z. T. Jiang, *J. Chem. Phys*., 2013, **138**, 094907.

25 W. T. Li, and D. Gersappe, *Macromolecules*, 2001, **34**, 6783-6789.

26 J. Z. Chen, C. X. Zhang, Z. Y. Sun, Y. S. Zheng, and L. J. An, *J. Chem. Phys*., 2006, **124**, 104907.

27 K. R. Shull, A. M. Mayes, and T. P. Russell, *Macromolecules*, 1993, **26**, 3929-3936.

28 K. R. Shull, *Macromolecules*, 1996, **29**, 2659-2666.

29 M. W. Matsen, *Macromolecules*, 1995, **28**, 5765-5773

30 T. Hashimoto, H. Tanaka, and H. Hasegawa, *Macromolecules*, 1990, **23**, 4378-4386.

31 K. A. Orso and P. F. Green, *Macromolecules*, 1999, **32**, 1087-1092.

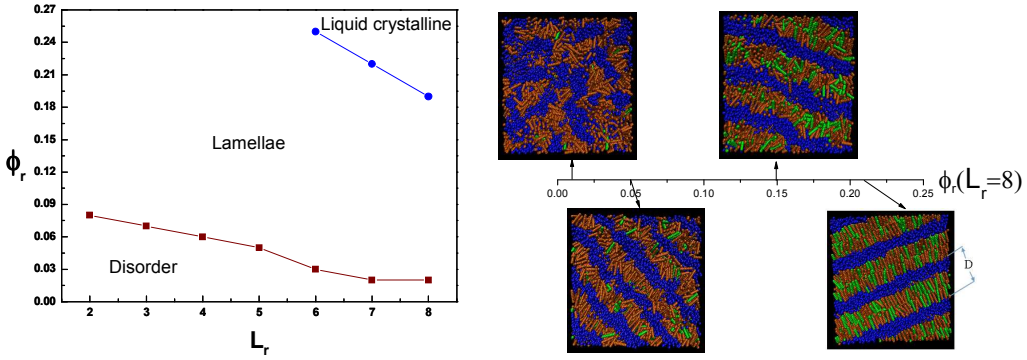

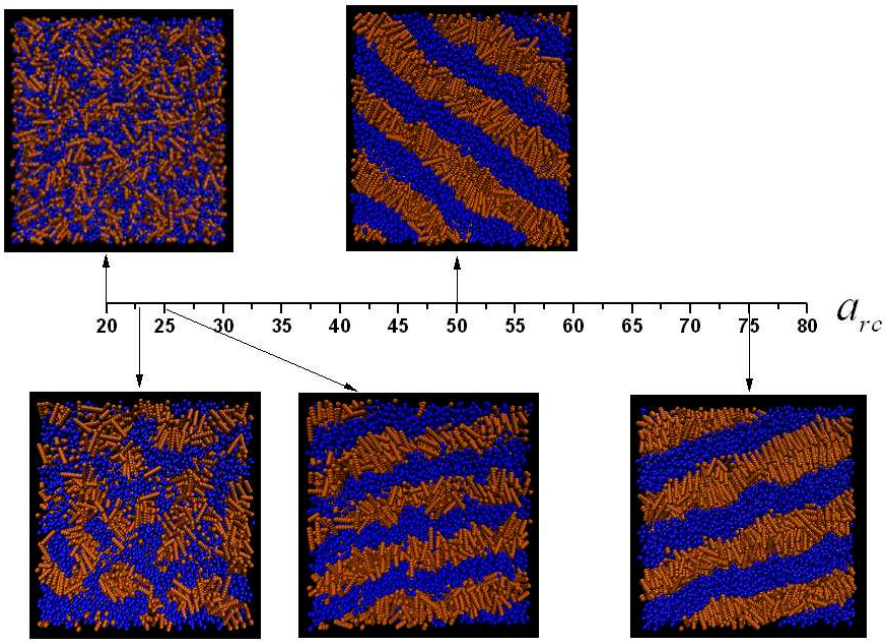

Fig.1 Representative simulated morphologies of R_8C_6 diblock copolymer melts with the increase of interactions a_{rc} .

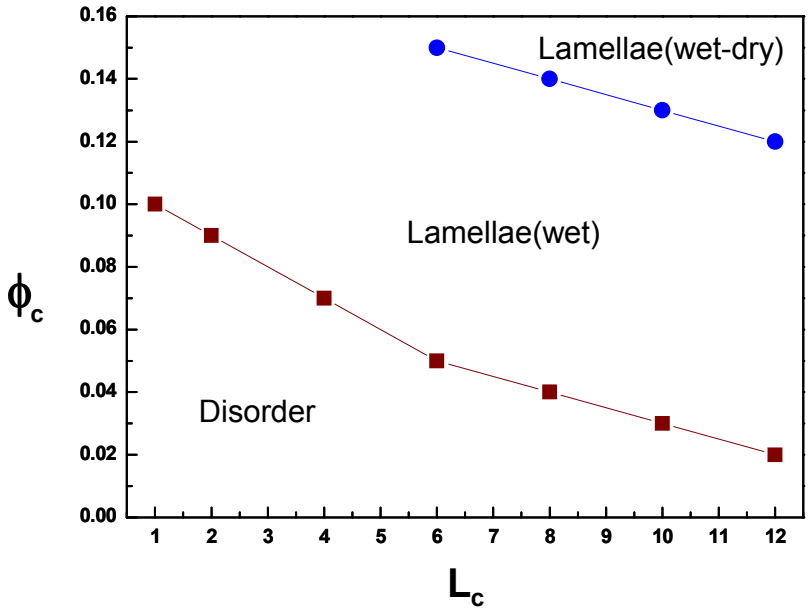

（a）

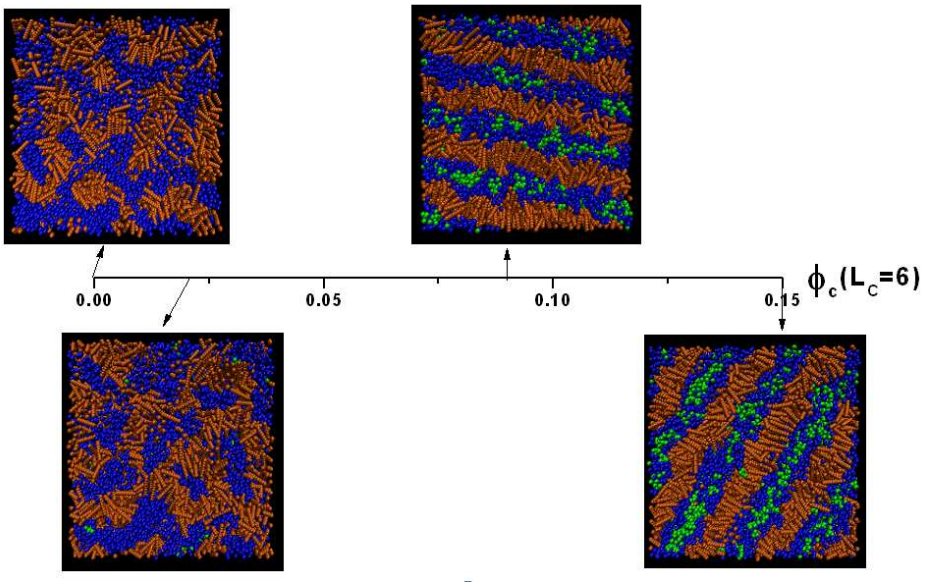

（b）

Fig.2（a）Phase diagram of rod-coil diblock copolymer/coil homopolymer blends for $a_{rc} = 23$ plotted in ϕ_c and L_c. （b）Simulated morphologies of R_8C_6/coil blends with L_c=6 and ϕ_c=0, 0.02, 0.09, and 0.15 , respectively.

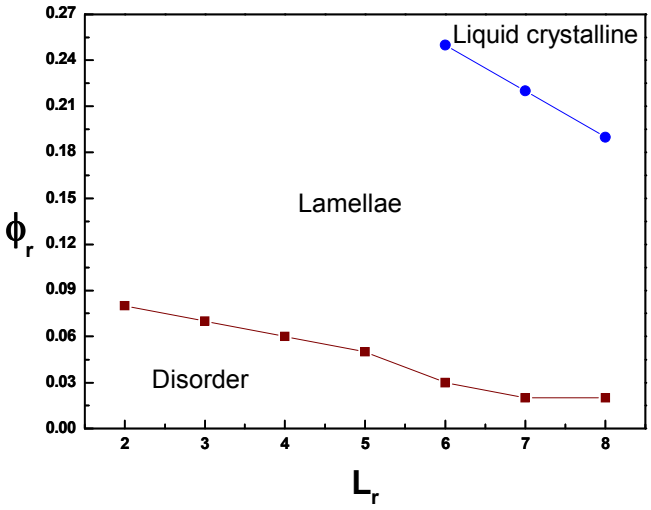

（a）

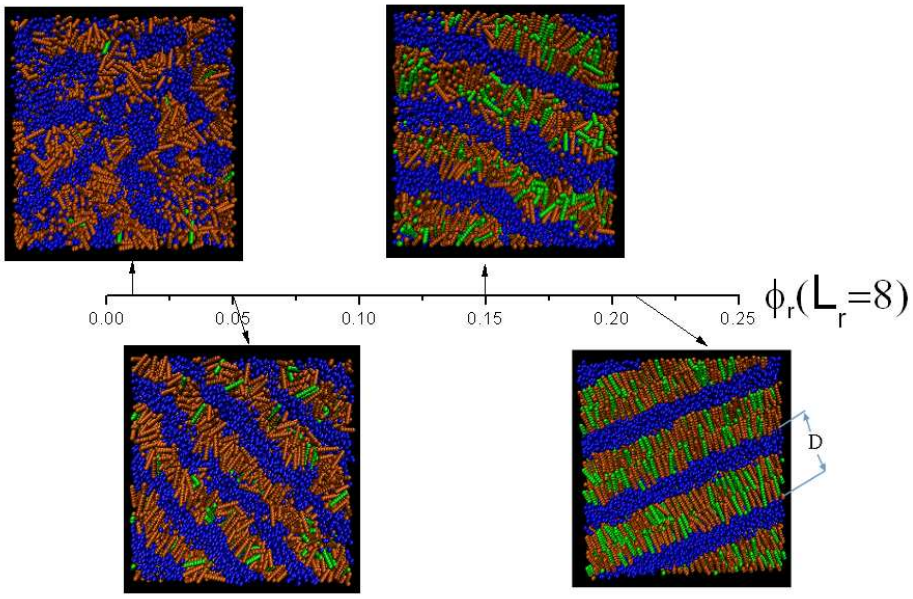

（b）

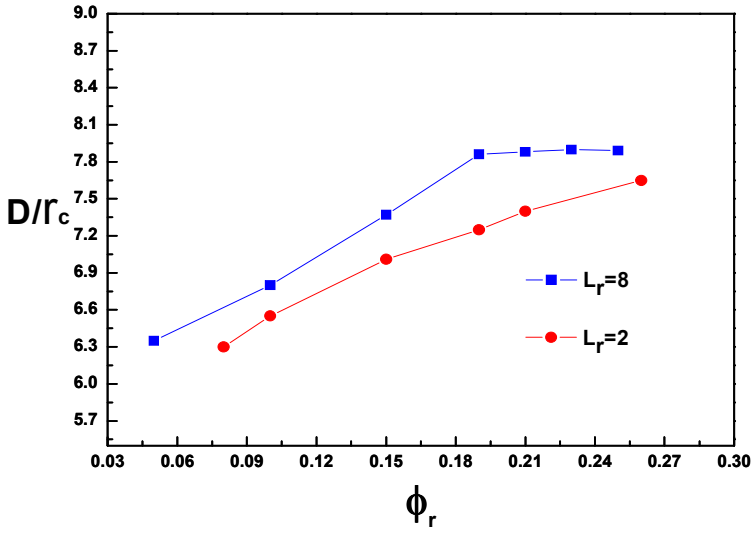

（c）

Fig.3 （a）Phase diagram of rod-coil/rod blends for $a_{rc} = 23$ plotted in ϕ_r vs L_r；(b) Simulated morphologies of blends with $L_r = 8$ and ϕ_r=0.01, 0.05, 0.15, and 0.21, respectively；(c) The lamellar spacing D versus ϕ_r for L_r=2 and 8，respectively.

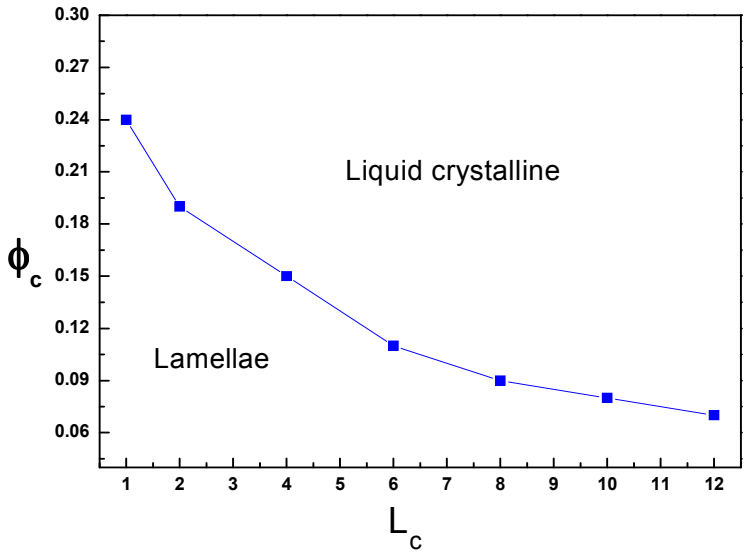

（a）

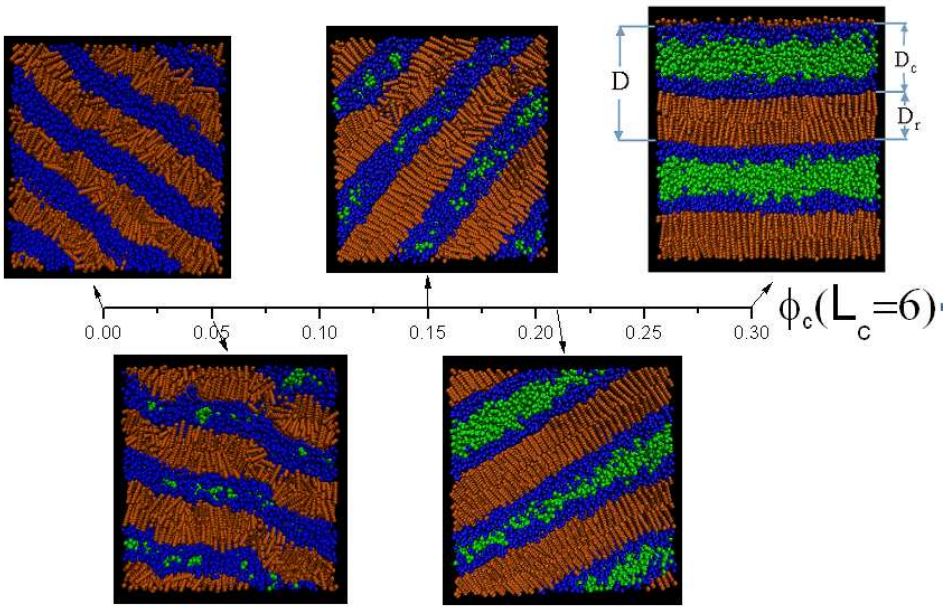

（b）

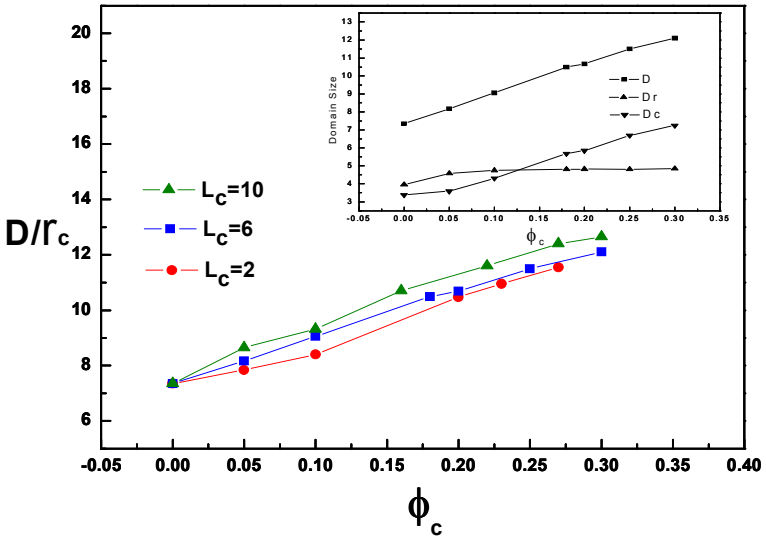

（c）

Fig.4（a）Phase diagram of rod-coil/coil blends for $a_{rc} = 50$；(b) Simulated morphologies of the blends with L_c=6 and ϕ_c= 0, 0.05, 0.15, 0.21, and 0.30, respectively; (c) The lamellar spacing D versus ϕ_c for L_c=2, 6, and10. The inset is the specific results for L_c=6 case, where D_c, D_r and D represent the domain spacing of coils, rods, and blends, respectively.

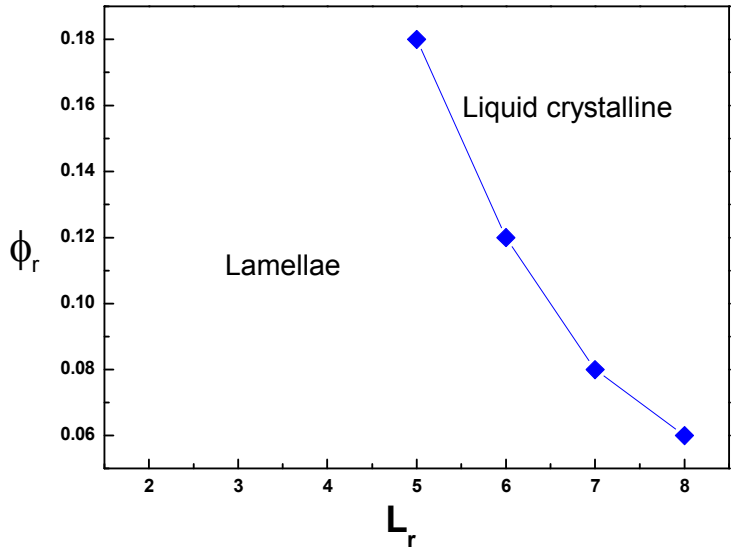

（a）

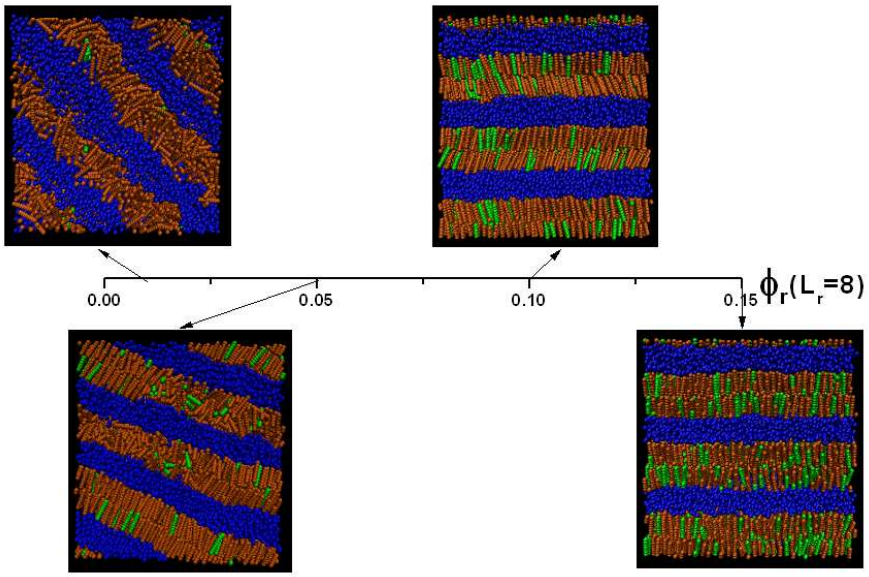

（b）

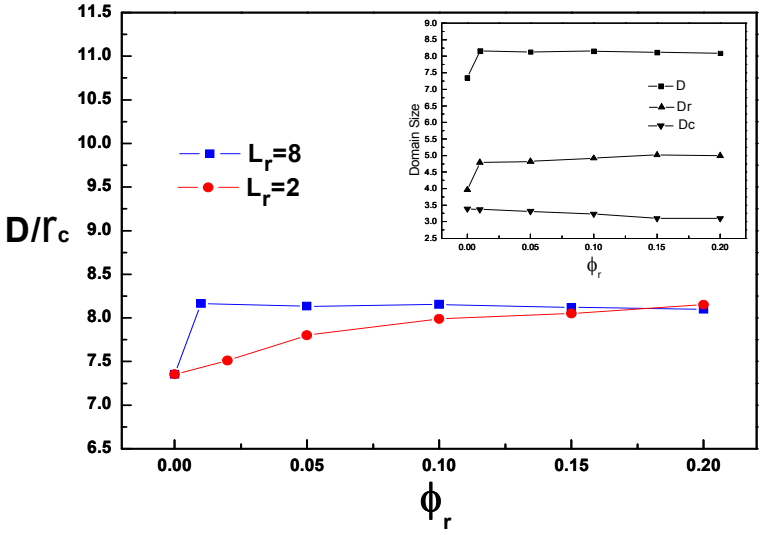

（c）

Fig.5 (a) Phase diagram of rod-coil/rod blends for $a_{rc} = 50$ plotted in ϕ_r vs L_r; (b) Simulated morphologies of blends with $L_r = 8$ and ϕ_r=0.01, 0.05, 0.10, and 0.15, respectively; (c) The lamellar spacing D versus ϕ_r for L_r=2 and 8，respectively (the inset is the results of L_r=8 case).

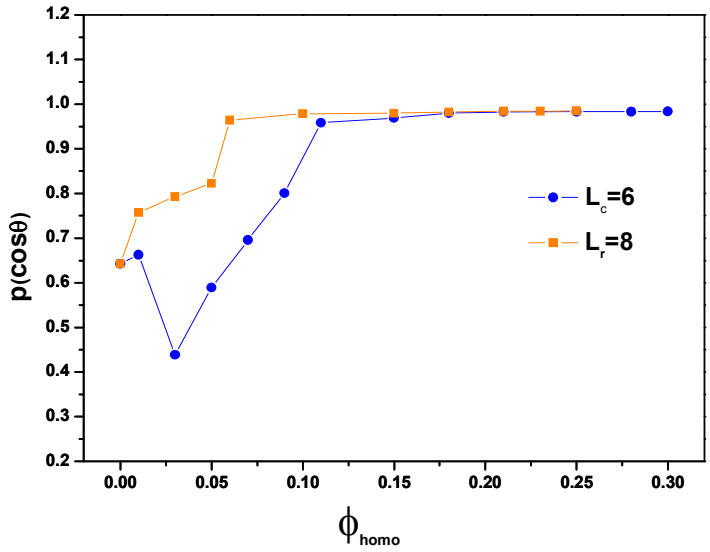

Fig.6 The rod orientation distribution $p(\cos\theta)$ versus the volume fraction of homopolymers, where θ is the included angle between two neighboring rods. Here $a_{rc} = 50$.